

Supporting Figures: Self-Assembly of Colloidal Nanocomposite Hydrogels Using 1D Cellulose Nanocrystals and 2D Exfoliated Organoclay Layers

T. Okamoto et al.

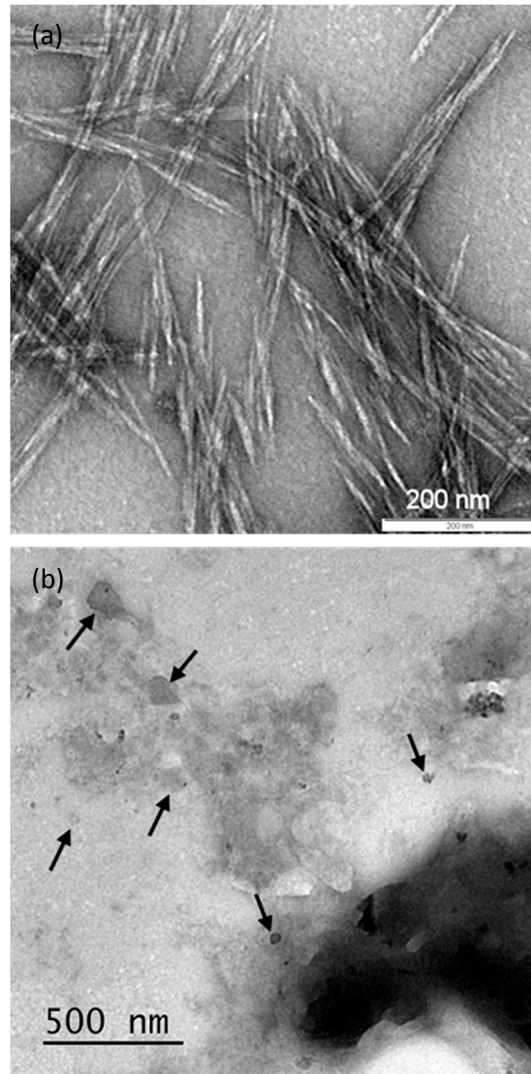


Figure S1: TEM images showing (a) uranyl acetate-stained cellulose nanocrystals (CNCs) and (b) exfoliated sheets of aminopropyl-functionalized magnesium phyllosilicate clay, indicated by arrows.

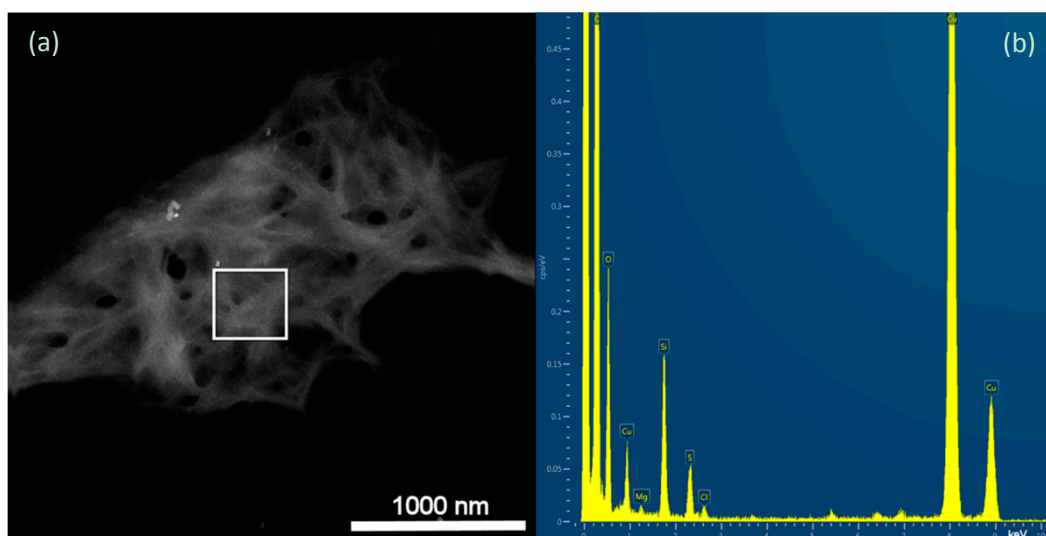


Figure S2: (a) High-angle annular dark-field STEM image of CNC–organoclay hydrogel sample; square box shows the area selected for EDX analysis; (b) EDX analysis of a corresponding gel sample.

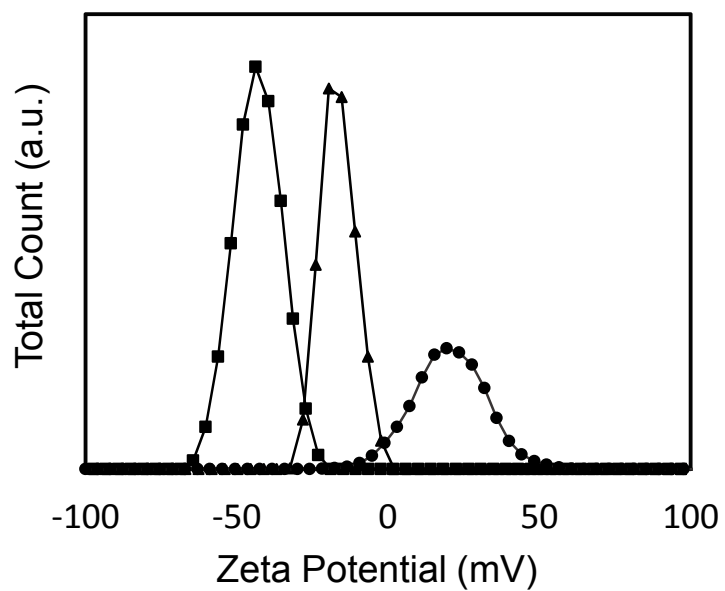


Figure S3: Zeta-potential profiles for CNCs (squares), freshly exfoliated organoclay sheets (circles), and a CNC–organoclay hydrogel dispersion (triangles).

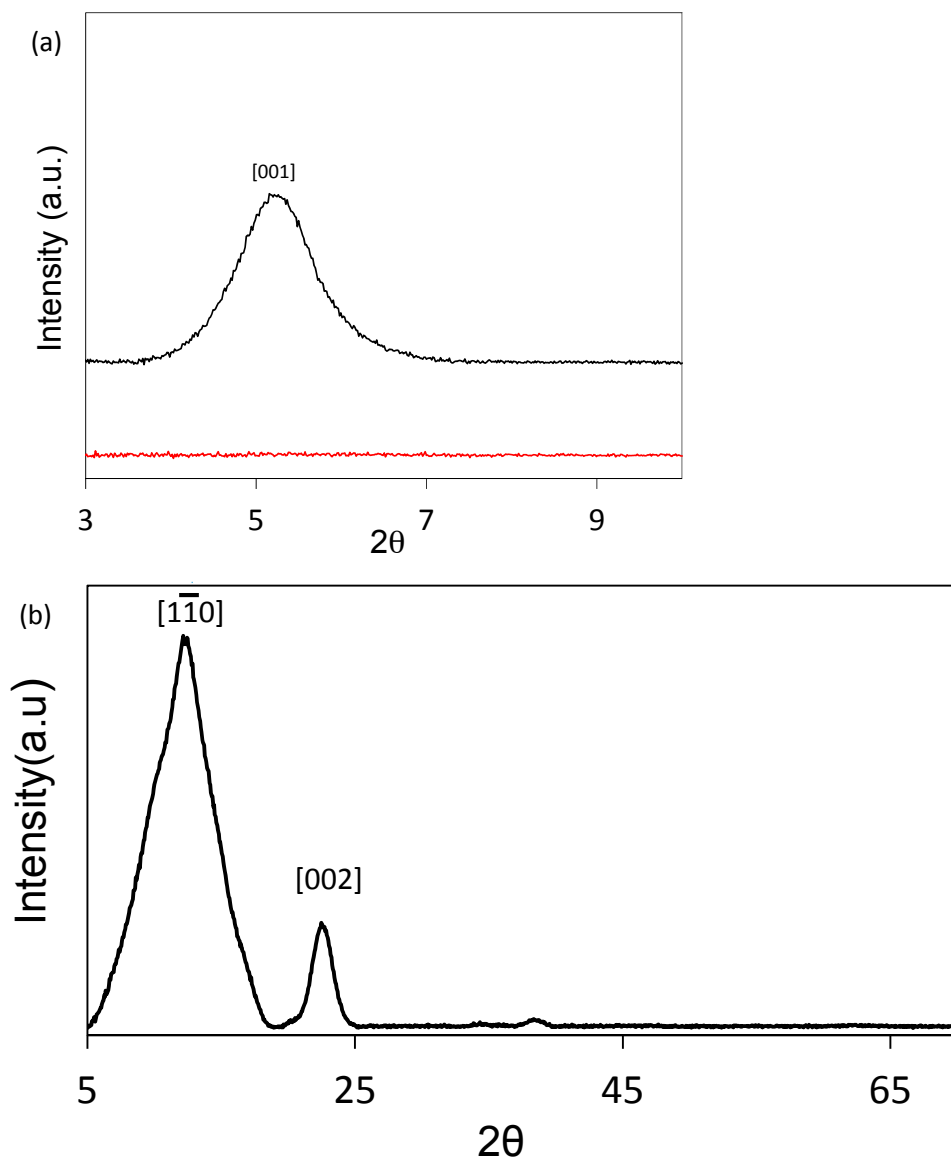


Figure S4: (a) Low-angle PXRD patterns of as-synthesized organoclay (black) and CNC-organoclay nanocomposite hydrogel (red), (b) high-angle PXRD pattern of CNC-organoclay nanocomposite hydrogels showing $[\bar{1}10]$ and [002] reflections associated with CNCs.

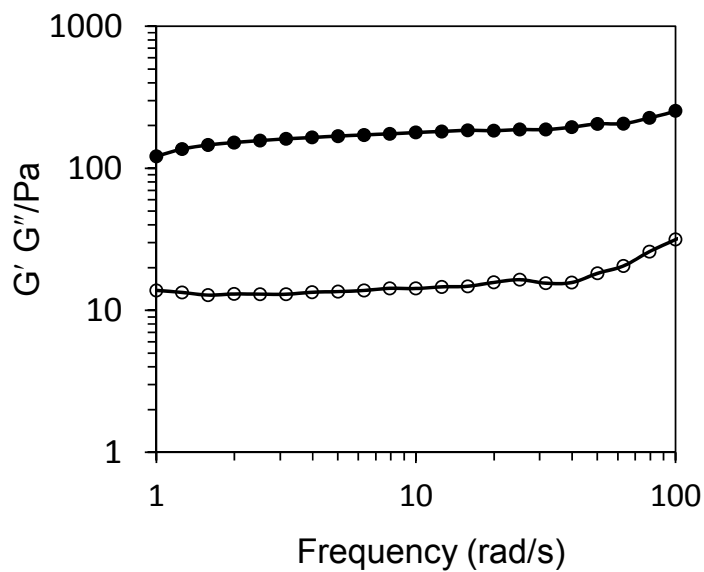


Figure S5: Frequency sweep profile showing storage G' (filled circles) and loss G'' moduli (open circles) of CNC-organoclay-ibuprofen nanocomposite hydrogel.

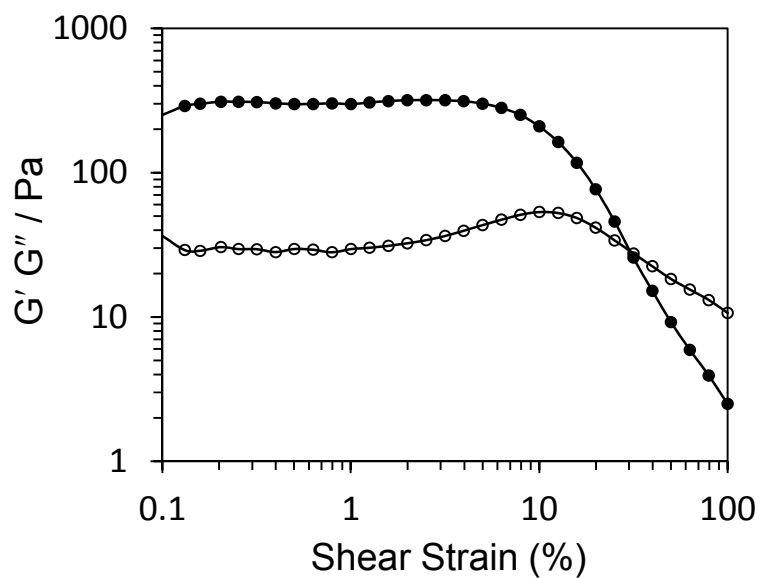


Figure S6: Oscillatory amplitude sweep curves showing storage G' (filled circles) and loss G'' moduli (open circles) at a constant frequency of 1 Hz for CNC-organoclay-ibuprofen hybrid hydrogel.